Annular Poiseuille flow of ER and MR materials

Henri P. Gavin
Department of Civil and Environmental Engineering, Duke University, Durham, NC 27708–0287
(June 8, 2001)

Accepted for Publication *Journal of Rheology.*

Electro- and magneto-rheological materials exhibit substantial increases in yield stress when subjected to strong electric or magnetic fields. The applied electric/magnetic field satisfies Laplace's equations in the ER/MR material. In annular geometries, the resulting spatial variation of the electric/magnetic field results in a yield stress inhomogeneity. The analysis of annular Poiseuille flow of ER/MR materials herein assumes a power-law relationship between the field and the yield stress, and includes the effects of the inhomogeneous yield stresses and hyperbolic shear stress distributions. The approximation of the solution to this problem by flow through an appropriately-defined rectangular duct (in which the yield stress is constant and the shear stresses are linearly distributed) can be remarkably accurate, even for non-slender ducts.

I. INTRODUCTION

Controllable hydraulic devices, in which the dissipation rate can be arbitrarily adjusted, are enabling new technologies for automation, vibration suppression and shock isolation in a wide range of industries. One approach to developing such devices makes use of electrorheological (ER) or magnetorheological (MR) materials. ER and MR materials are fluid suspensions of electrically or magnetically polarizeable particles, one to ten microns in diameter. Devices using these materials are easily manufactured, have no moving parts, and provide a direct transduction from an electrical control signal to a change in mechanical properties. The defining feature of ER and MR materials is that their constitutive behavior is sensitive to their electrostatic and magnetostatic environments, respectively (Parthasarathy *et al.* 1996, Rankin *et al.* 1998). When subjected to intense electric or magnetic fields (3-5 kV/mm or 0.5-1 Tesla) the yield stress and viscoelastic properties of these materials increase by orders of magnitudes (Gamota *et al.* 1991). The change in material properties occurs within milliseconds and is completely reversible upon removal of the field. The material behavior is conveniently modeled by the Bingham constitutive equation in which the yield stress is controllable. Some recent examples of the evolving nature of these materials include the work of U.S. Choi, *et al.* (2000), Huang *et al.* (1998), Phule *et al.* (1999), Trlica *et al.* (2000), Quist *et al.* (1999) and Wu *et al.* (1999). These materials are being applied to damping technologies (Burton *et al.* 1996, Gavin *et al.* 1996b, Gavin 1998, Kamath *et al.* 1996, Lindler *et al.* 1999, Marksmeier *et al.* 1999, Sims *et al.* 2000), seismic response suppression (Dyke *et al.* 1998, Gavin 2001), controllable vehicle suspensions (Choi, S.B., *et al.* 2000, Peel *et al.* 1996, Murata *et al.* 1999), and the control of rotor dynamics (Shimada *et al.* 2000, Yao *et al.* 2000, Kamath *et al.* 1999). In all of these applications, the electric/magnetic field lines are perpendicular to the flow's stream lines and the materials flow through slender annular spaces defined by the electrodes or magnetic circuit elements creating the field.

Several investigators have studied the axi-symmetric Poiseuille flow of Bingham materials (Wilkinson 1960, Bird *et al.* 1960, Bird *et al.* 1983). Nguyen and Boger (1992) describe potential sources of error in the rheometry of Bingham materials. In annular Poiseuille flow the shear stress distribution is hyperbolic and the yield stresses in ER/MR materials are inhomogeneous due to spatial variation of the electric/magnetic field. Atkin *et al.* (1991) studied the Couette and Poiseuille flow of ER materials in annular geometries for the case in which the yield stress increases quadratically with the electric/magnetic field. These and other analyses of the annular Poiseuille flow problem of Bingham and ER/MR materials require a numerical method to solve the boundary value problem (Bird *et al.* 1983, Rajagopal *et al.* 1992, Atkin 1991). In some studies, a rectangular duct approximates the unwrapped annular geometry obviating the consideration of the field inhomogeneity, the yield stress inhomogeneity, the hyperbolic variation of the shear stresses (Makris *et al.* 1996, Peel *et al.* 1996, Rajagopal *et al.* 1992). ER/MR devices are commonly designed using such approximations (Burton *et al.* 1996, Gavin 1998, Lindler *et al.* 1999).

This paper provides a comparison of an analytical solution to the rectangular duct flow of homogeneous Bingham materials to the exact solution for inhomogeneous ER/MR materials in annular Poiseuille flow. Inhomogeneity of material properties arises from the nonuniform electric/magnetic field due to the annular geometry and from particulate migration across the flow direction due to electro/magneto-phoretic effects and the inertial lift forces on particulates in a shear flow near a wall. These inertial lift forces may dramatically lower the concentration of particulates (and the yield stress) near the walls and effectively provides an upper bound to the pressure gradients developed along ducts of flowing ER/MR materials. A statistical comparison of continuum models incorporating the inhomogeneities due to particulate migration with measurements of pressure gradients in flowing ER materials illustrates that the assumption of homogeneity provides an upper bound to pressure gradients achievable in these materials (Gavin 1997).

This paper focuses on the inhomogeneity of the ER/MR material properties arising from the nonuniform electric/magnetic field in annular ducts. The annular duct is a common geometry for ER/MR devices, however, these devices are typically analyzed and designed using a rectangular duct approximation for the duct geometry. It is seen that the rectangular duct analogy can lead to errors as great as one hundred percent when the field inhomogeneity is neglected. An appropriately defined analogous rectangular duct problem is presented which accurately represents the inhomogeneous annular Poiseuille flow problem. The errors associated with the rectangular duct approximation presented in this paper are extremely small, even for non-slender annuli.

II. MATERIAL AND FIELD PROPERTIES

In this and following sections, the electric/magnetic field is simply referred to as the *field*, whereas the velocity field is simply referred to as the *flow*. The material yield stress is assumed to be proportional to the n-th power of the field, and the cases $n = 0$, $n = 1$, and $n = 2$ are described in detail. Assuming point electro-static dipole interactions between the particles of an ER suspension, n equals 2 exactly. As the dipole moment reaches a saturation level, the yield stress approaches a linear relationship with the field (Rankin *et al.* 1998). For MR materials approaching magnetic saturation, $n = 3/2$ (Ginder *et al.* 1996). A general power-law relationship between the field and the yield stress is therefore chosen to model the variable sensitivity of the yield stress to the field.

An idealized ER or MR fluid resists shear stress with a field dependent yield stress, ${\tau_y}^*(\mathcal{F}^*)$, and a viscous stress proportional to the shear rate, $\dot{\gamma}_{xr}$. (The asterisk indicates dimensional quantities.) This behavior motivates the use of the Bingham constitutive equation (Parthasarathy *et al.* 1996),

$$\tau^*(\dot{\gamma}_{xr}, \mathcal{F}^*) = {\tau_y}^*(\mathcal{F}^*)\mathrm{sgn}\dot{\gamma}_{xr} + \eta^*\dot{\gamma}_{xr}. \tag{1}$$

Pre-yield deformations are neglected in the Bingham material model, and the plastic viscosity, η^*, is assumed to be independent of the applied field. The relationship between the yield stress and the field is approximated by a power law

$${\tau_y}^*(\mathcal{F}^*) = S^*(\mathcal{F}^*)^n. \tag{2}$$

The material constants S^*, n, and η^* are typically obtained through Couette rheometry. The exponent n is zero for a field-insensitive Bingham material and ranges from 0 and 2 for ER and MR materials (Parthasarathy *et al.* 1996, Ginder *et al.* 1996). The exponent n approaches 0 in MR materials in which the magnetization of the particulates nears saturation.

If there is no electrical charge within the annulus and the permittivity/permeability properties within the annulus are uniform and insensitive to flow, the field, $\mathcal{F}^*$, satisfies $\mathcal{F}^*(r^*) = -\nabla\mathcal{E}^*$, where the Laplacian of the potential, $\nabla^2\mathcal{E}^* = 0$, with appropriate boundary conditions. In alternating or rapidly changing fields, the fields will be governed by Maxwell's equations, and constitutive models describing these effects on the behavior of ER materials have been formulated (Rajagopal and Růžička, 1996). In the present analysis, we assume that the electric/magnetic field is held constant and we neglect perturbations in the applied fields due to the motion of the polarized particulates. Further we neglect any conduction currents in the electric field, which is more appropriate for anhydrous ER materials.

In an annular geometry the field is proportional to $1/r^*$.

$$\mathcal{F}^*(r^*) = V^*\frac{1}{r^*}, \tag{3}$$

where $V^* = \mathcal{E}^*/\log(R_1^*/R_2^*)$ and $\mathcal{E}^*$ is the potential difference between the inner wall ($r^* = R_1^*$) and the outer wall ($r^* = R_2^*$).

In the following analysis, the radius is normalized by the radius of the outer wall, $r = r^*/R_2^*$. The slenderness of the annulus is defined by $R = R_1^*/R_2^*$, and $R \leq r \leq 1$ within the annulus. The shear stress is normalized by the yield stress at the outer radius, $\tau_{xr} = \tau^*(R_2^*)^n/(S^*(V^*)^n)$, the dimensionless yield stress is $\tau_y = {\tau_y}^*(R_2^*)^n/(S^*(V^*)^n) = 1/r^n$, and the dimensionless plastic viscosity is $\eta = \eta^*(R_2^*)^n/(S^*(V^*)^n)$. Using these dimensionless variables, the Bingham constitutive equation is

$$\tau_{xr}(\dot{\gamma}_{xr}) = r^{-n} + \eta\dot{\gamma}_{xr}. \tag{4}$$

While the Bingham model does not capture all the complex mechanisms of ER and MR materials, it provides for simple approximations describing the flow of these materials, expressions which are sufficiently accurate for design purposes (Gavin *et al.* 1996a). In applications in which the flow is oscillatory, the pre-yield viscoelastic properties of the materials can significantly affect their behavior (Gamota *et* *al.* 1991, Gavin 2001). The visco-elastic behavior of ER/MR materials is rich in relaxation mechanisms, including characteristic times associated with polarization, particle aggregation, and the bulk modulus, viscosity and inertia of the dispersant. A frame-indifferent constitutive model capturing the pre- and post-yield behaviors has been formulated (Wineman and Rajagopal, 1995). Such complete descriptions involve material constants and relaxation functions which, as yet, have not been experimentally evaluated. Even so, the force capacity of a device can be accurately predicted from the analysis of quasi-steady flow (Gavin *et al.* 1996a).

The Dirichlet boundary conditions in this problem are homogeneous, and the stresses and velocities in a homogeneous generalized Newtonian fluid can be expressed explicitly as a function of the pressure gradient and geometry and are material independent. Furthermore, when the Poiseuille flow problem is cast using the dimensionless variables presented in this paper, the rectangular duct approximation to annular Poiseuille flow can be very accurate, even for non-slender annuli ($R \approx 0.2$).

III. ANNULAR POISEUILLE FLOW OF ER AND MR MATERIALS

Figure 1 illustrates the distribution of fields in a ER/MR material flowing through an annular duct with inner radius R and outer radius 1. The total flow rate Q is diagrammatically represented on the left and the velocity is in the positive x direction, as shown. The electric field intensity, $\mathcal{F}(r)$ (a), is given by equation (3), and is higher at the inner duct wall. Because the yield stress increases monotonically with $\mathcal{F}(r)$, the yield stress, illustrated as dotted lines in part (b) of the figure, is also greater at the inner duct wall. The shear stress follows

$$\frac{\partial \tau_{xr}}{\partial r} + \frac{\tau_{xr}}{r} = \frac{\partial p}{\partial x}, \tag{5}$$

subjected to no-slip conditions at the walls. Equation (5) has the solution

$$\tau_{xr}(r) = -\frac{1}{2}p'r + \frac{D}{r}, \tag{6}$$

where x is in the axial direction, $p' = -\partial p/\partial x$ is the constant pressure gradient, and the constant D is determined from the boundary conditions. In flowing ER/MR materials, the shear stresses exceed the yield stress in the regions $r < r_1$ and $r > r_2$ as shown in part (b) of Fig. 1. The shear rate $\gamma_{xr}(r)$ (c) follows from the constitutive relation (4) and is zero in the region $r_1 < r < r_2$. The flow velocity profile, $u_x(r)$ (d) for annular Poiseuille flow of ER/MR materials is obtained by integrating $\gamma_{xy}(r)$ with no-slip boundary conditions.

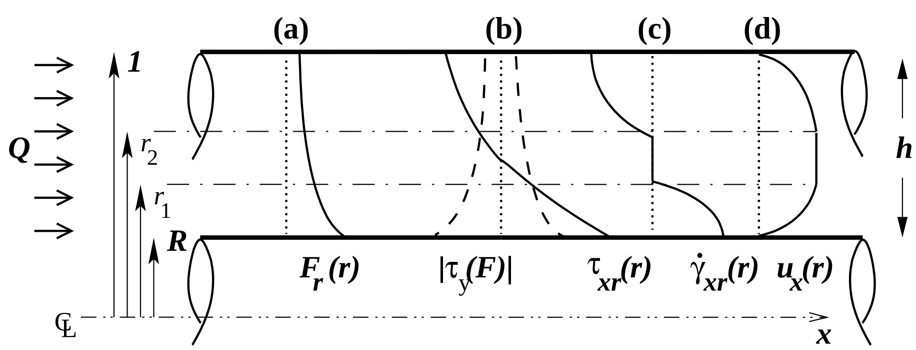

FIG. 1. Distribution of electric/magnetic, stress, and flow fields in annular Poiseuille flow of ER/MR materials. (a): Field $\mathcal{F}$; (b): yield stress, $\tau_{\rm y}(\mathcal{F})$ and shear stress, $\tau_{\rm y}(r)$; (c): shear rate $\dot{\gamma}_{xr}(r)$; and (d): flow velocity $u_x(r)$.

The two homogeneous Dirichlet conditions, $u_x(R) = 0$ and $u_x(1) = 0$ can be expressed as a definite integral

$$\int_R^1 \frac{\partial u_x}{\partial r} dr = 0, \tag{7}$$

and for a generalized Newtonian fluid, the shear stress is an anti-symmetric single valued function of the velocity gradient

$$\tau_{xr}\left(\frac{\partial u_x}{\partial r}\right) = -\tau_{xr}\left(-\frac{\partial u_x}{\partial r}\right). \tag{8}$$

Equations (7) and (8) imply that

$$\int_R^1 \tau_{xr}\left(\frac{\partial u_x}{\partial r}\right) dr = 0. \tag{9}$$

Substituting equation (6) into equation (9) and solving for D,

$$D = \frac{p'}{4}\,\frac{1 - R^2}{\log R}. \tag{10}$$

The effect of the annular geometry is captured by the constant D. As D approaches zero, the distribution of shear stresses across the duct becomes linear, which is the case in rectangular duct flow. While D is independent of material properties and applies to any generalized homogeneous Newtonian fluid flowing through annular ducts, equation (10 can not be directly applied to ER or MR materials in annular geometries. In the annular Poiseuille flow of ER/MR materials, the yield stress and shear rates vary spatially and the symmetry of equation (8) is lost. As will be seen in the next section, equation (10) is accurate only for very slender ducts and for flows with a high dimensionless pressure gradient. Dimensional forms for D and p' are $D^* = DS^*(V^*/R_2^*)^n$ and $p'^* = p'S^*(V^*)^n/(R_2^*)^{n+1}$. The yield stress exceeds the shear stress within a region near the center of the annulus. The radial coordinates r_1 and r_2 define the region of unyielded, un-shearing material, $\tau_{xr}(r_1) = \tau_{\rm y}(r_1) = r_1^{-n}$, $\tau_{xr}(r_2) = -\tau_{\rm y}(r_2) = -r_2^{-n}$, and $|\tau_{xr}(r)| \le r^{-n}$ for $r_1 \le r \le r_2$, as shown in Fig. 1. Substituting equation (6) into the two equality conditions above leads to two independent polynomials for the coordinates r_1 and r_2. The flow velocity profile comprises three piece-wise continuous functions. In the region $r_1 \le r \le r_2$, $u_x(r)$ is constant. In the region $R \le r \le r_1$, the velocity gradient is

$$\frac{\partial u_{x1}}{\partial r} = \frac{\tau_{xr}(r) - r^{-n}}{\eta}, \tag{11}$$

and in the region $r_2 \le r \le 1$,

$$\frac{\partial u_{x2}}{\partial r} = \frac{\tau_{xr}(r) + r^{-n}}{\eta}. \tag{12}$$

Three cases are considered in this section: $n = 0$, $n = 1$, and $n = 2$. For each of these cases r_1 and r_2 are expressed as closed form functions of D and p'. The constant D is calculated numerically by applying the Dirichlet conditions $u_x(R) = 0$, $u_x(1) = 0$, and $u_x(r_1) = u_x(r_2)$. The volumetric flow rate is found by integrating the velocity profile, and the critical pressure gradient required to initiate flow, p'_{cr} is computed by setting τ_{xr} equal to 1 at $r = R$ and at $r = 1$.

A. Case 1: $n = 0$

This case corresponds to an ordinary Bingham material, in which the yield stress does not depend on the field, inhomogeneous or otherwise. At $r = r_1$, $\tau_{xr}(r_1) = 1$ and $-\frac{1}{2}p'r_1 + D/r_1 = 1$; at $r = r_2$, $\tau_{xr}(r_2) = -1$, and $-\frac{1}{2}p'r_2 + D/r_2 = -1$. The meaningful roots to these two quadratic equations in r_1 and r_2 are

$$r_{1,2} = \frac{1}{p'}\left(\sqrt{1 + 2p'D} \mp 1\right). \tag{13}$$

Integrating the velocity gradient in $R \leq r \leq r_1$ gives

$$u_{x1}(r) = \frac{1}{\eta}\left[-\frac{p'}{4}(r^2 - R^2) + D\log\left(\frac{r}{R}\right) - (r - R)\right], \tag{14}$$

and integrating the velocity gradient in $r_2 \leq r \leq 1$ gives

$$u_{x2}(r) = \frac{1}{\eta}\left[-\frac{p'}{4}(r^2 - 1) + D\log r + r - 1\right]. \tag{15}$$

Setting $u_{x1}(r_1) = u_{x2}(r_2)$, and simplifying, leads to

$$\frac{p'}{4}(r_1^2 - r_2^2 - R^2 + 1) + D\log\left(\frac{r_2 R}{r_1}\right) + r_1 + r_2 - R - 1 = 0, \tag{16}$$

where r_1 and r_2 are the functions of p' and D given in equation (13). The volumetric flow rate is calculated from the piece-wise continuous flow velocity profile (Wilkinson 1960),

$$Q = -\pi\left[\int_R^{r_1} r^2\frac{\partial u_{x1}}{\partial r}dr + \int_{r_2}^1 r^2\frac{\partial u_{x2}}{\partial r}dr\right], \tag{17}$$

and for the case $n = 0$,

$$Q = -\frac{\pi}{\eta}\left[-\frac{p'}{8}(r_1^4 - r_2^4 - R^4 + 1) + \frac{D}{2}(r_1^2 - r_2^2 - R^2 + 1) - \frac{1}{3}(r_1^3 + r_2^3 - R^3 - 1)\right]. \tag{18}$$

The critical pressure gradient is $p'_{cr} = 2/(1 - R)$.

B. Case 2: $n = 1$

In this case the ER/MR material exhibits a yield stress which is proportional to the field. The dimensionless form of the yield stress is therefore $1/r$. At $r = r_1$, $-\frac{1}{2}p'r_1 + D/r_1 = 1/r_1$, and at $r = r_2$, $-\frac{1}{2}p'r_2 + D/r_2 = -1/r_2$. Proceeding as in the previous case,

$$r_{1,2} = \sqrt{\frac{2}{p'}(D \mp 1)}, \tag{19}$$

$$u_{x1}(r) = \frac{1}{\eta}\left[-\frac{p'}{4}(r^2 - R^2) + (D - 1)\log\left(\frac{r}{R}\right)\right], \tag{20}$$

$$u_{x2}(r) = \frac{1}{\eta}\left[-\frac{p'}{4}(r^2-1) + (D+1)\log r\right], \tag{21}$$

$$\frac{p'}{4}(r_1^2 - r_2^2 - R^2 + 1) + (D-1)\log\left(\frac{r_2 R}{r_1}\right) = 0, \tag{22}$$

and

$$Q = \frac{\pi}{8\eta}\left[p'(r_1^4 - r_2^4 - R^4 + 1) - 4(D-1)(r_1^2 - R^2) - 4(D+1)(1-r_2^2)\right]. \tag{23}$$

The pressure gradient required to initiate flow is $p'_{cr} = 4/(1-R^2)$.

C. Case 3: $n = 2$

In this case the yield stress of the ER/MR material increases quadratically with the field. The dimensionless form of the yield stress is now $1/r^2$. At $r = r_1$, $-(1/2)p'r_1 + D/r_1 = 1/r_1^2$, and at $r = r_2$, $-(1/2)p'r_2 + D/r_2 = -1/r_2^2$. Following the method of the previous two cases,

$$r_{1,2} = 2\sqrt{\frac{2D}{3p'}}\cos\left(\frac{1}{3}\arccos\left(\mp\left(\frac{3}{2}\right)^{3/2}\sqrt{\frac{p'}{D^3}}\right)\right), \tag{24}$$

$$u_{x1}(r) = \frac{1}{\eta}\left[-\frac{p'}{4}(r^2 - R^2) + D\log\left(\frac{r}{R}\right) + \left(\frac{1}{r} - \frac{1}{R}\right)\right], \tag{25}$$

$$u_{x2}(r) = \frac{1}{\eta}\left[-\frac{p'}{4}(r^2-1) + D\log r - \left(\frac{1}{r}+1\right)\right], \tag{26}$$

$$\frac{p'}{4}\left[(r_1^2 - r_2^2 - R^2 + 1) - D\log\left(\frac{r_2 R}{r_1}\right) + \frac{1}{r_2} - \frac{1}{r_1} - \frac{1}{R} - 1\right] = 0, \tag{27}$$

and

$$Q = \frac{\pi}{8\eta}\left[p'(r_1^4 - r_2^4 - R^4 + 1) - 4D(r_1^2 - r_2^2 - R^2 + 1) + 8(r_1 + r_2 - R - 1)\right]. \tag{28}$$

The pressure gradient required to initiate flow is $p'_{cr} = 2/(R^2 - R)$.

Figure 2 illustrates the numerical solution to equations (16), (22), and (27) for the root D as a function of R and p'. At high pressure gradients and shear rates, viscous stresses are dominant, and ER/MR materials resemble homogeneous Newtonian fluids consistent with equations (8) and (10). in Fig. 2. Equation (10) closely approximates the numerical solutions for $n = 0$, for $R > 0.5$, or for $p' > 100$. For these parameters, the rectangular duct approximation for the flow of ER/MR materials should not give rise to significant errors. It should be noted, however, that in ER/MR flows in which the controllable yield stresses, $\tau_y(\mathcal{F}$ are significantly greater than the viscous stresses $\eta\dot{\gamma}_{xr}$, the dimensionless pressure gradient p' is small and equation (10) should not be used.

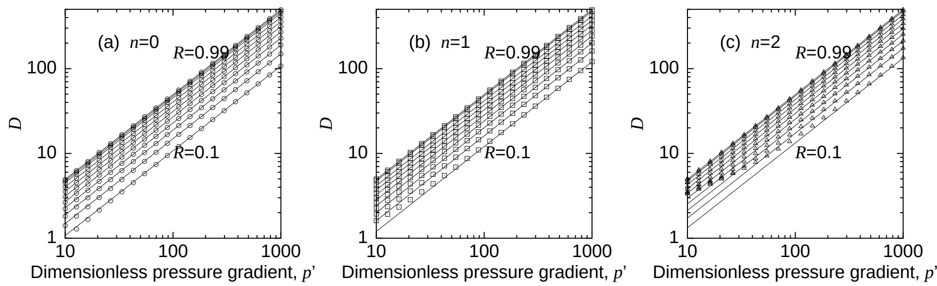

FIG. 2. Solution to equations (16), (22), and (27) as a function of p' and R. Symbols: roots of equations (16), (22), and (27). Lines: equation (10). $R = 0.1$, 0.2, 0.3, 0.4, 0.5, 0.6, 0.7, 0.8, 0.9, 0.95, and 0.99.

IV. ACCURACY OF APPROXIMATE POISEUILLE FLOW SOLUTIONS

In the design of ER and MR devices for Poiseuille flow, it is typically assumed that the field and yield stress are homogeneous and that the shear stress varies linearly across the annulus. These approximations are representative of Poiseuille flow of Bingham materials through ducts with rectangular cross sections and are commonly used to approximate ER/MR behavior in annular geometries (Burton *et al.* 1996, Jolly 1999, Gavin 1998, Kamath 1996).

When the field-generating surfaces (i.e. electrodes) are parallel and flat, the field is uniform. Therefore, the Poiseuille flow of ER and MR materials through rectangular ducts is no different than for ordinary, homogeneous, Bingham materials, (Wilkinson 1960, Bird *et al.* 1960, Bird *et al.* 1983, Phillips 1969). The solution for the Poiseuille flow of Bingham materials through a rectangular gap used here was proposed by Phillips (1969), and is expressed in polynomial form as

$$P^3 - (1 + 3T)P^2 + 4T^3 = 0, \tag{29}$$

where the dimensionless terms are $P = p'/p'_N$ and $T = \tau_{\rm y}/(p'_N h)$, h is the distance between the walls of the duct, and p'_N is the pressure gradient of a Newtonian fluid flowing through the duct at a flow rate Q. The quantity P has physical significance as the factor by which the resistance to steady flow increases when the field is applied to the ER/MR material. The meaningful roots to equation (29) are

$$P(T) = \frac{2}{3}(1 + 3T)\left[\cos\left(\frac{1}{3}\arccos\left(1 - 54\left[\frac{T}{1 + 3T}\right]^3\right)\right) + \frac{1}{2}\right]. \tag{30}$$

and, inversely,

$$T(P) = P\cos\left(\frac{1}{3}\arccos\left(\frac{1}{P} - 1\right) + \frac{4\pi}{3}\right). \tag{31}$$

In order to approximate the flow of ER/MR materials through an annulus, using equation (30), $h = 1 - R$ and

$$p'_N = \frac{8\eta Q}{\pi}\left[1 - R^4 + \frac{(1 - R^2)^2}{\log R}\right]. \tag{32}$$

In Fig. 3, 4, and 5, solutions for the cases $n = 0$, $n = 1$, and $n = 2$ are compared to equation (30) for annulus geometries $R = 0.1$,0.2,...,0.9,0.95, and 0.99, and pressure gradients ranging from $p' = p'_{cr}$ to $p' = 100p'_{cr}$. For each value of R and p', equations (16), (22), and (27) are solved numerically for D. Flow rates from equations (18), (23), and (28) are used in equation (32) to compute p'_N, and the non-dimensional groups for annular flow are calculated as $\hat{P}(R, p') = p'/p'_N$ and $\hat{T}(R, p') = \hat{\tau}_y/(p'_N(1-R))$. Three values for the *effective yield stress*, $\hat{\tau}_y$ are investigated: the yield stress at the inner wall $\hat{\tau}_y = 1/R^n$, at mid-annulus $\hat{\tau}_y = (2/(R+1))^n$, and at the outer wall $\hat{\tau}_y = 1$. In all cases the annular and rectangular duct solutions converge as R approaches 1.

The relative errors, e, of the rectangular duct approximations are calculated using equation (33) and are shown in Fig. 6.

$$e(R) = \frac{\left[\sum_i [\hat{P}(R, p'_i) - P(\hat{T}(R, p'_i))]^2\right]^{1/2}}{\left[\sum_i [\hat{P}(R, p'_i)]^2\right]^{1/2}}, \tag{33}$$

where $P(\hat{T})$ is calculated from equation (30).

When $\hat{\tau}_y = (2/(1+R))^n$ equation (30) remains accurate for non-slender ducts. If the yield stress is evaluated at the inner radius, ($\hat{\tau}_y = 1/R^n$), or the outer radius ($\hat{\tau}_y = 1$), very slender ducts ($R \geq 0.99$) are required in order for equation (30) to accurately represent the annular Poiseuille flow of ER and MR materials. If the effective yield stress is evaluated at mid-duct, $\hat{\tau}_y = (2/(R+1))^n$, and $n = 1$ or $n = 0$, equation (30) approximates the numerical solution of the flow through the annulus to within one percent, even for annular ducts with non-slender geometries, as is shown in Fig. 6.

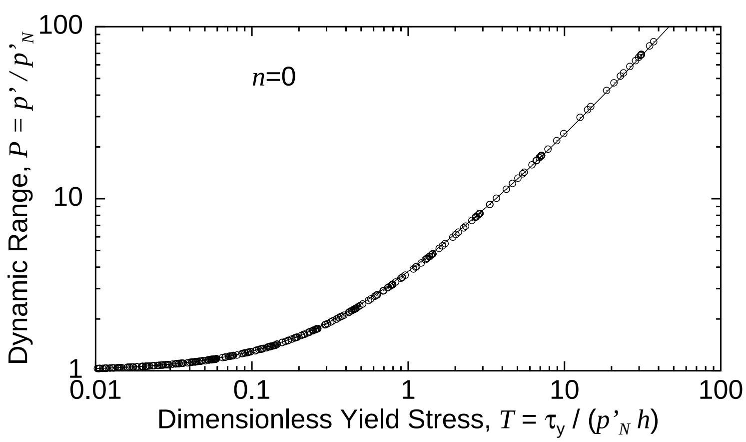

FIG. 3. Poiseuille flow of ER and MR materials through rectangular ducts (solid line) and annular ducts (symbols: $n = 0$ and $0.1 \leq R \leq 0.99$).

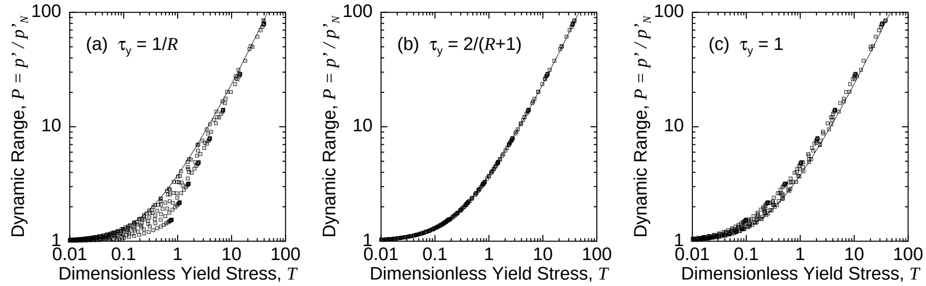

FIG. 4. Poiseuille flow of ER and MR materials through rectangular ducts (solid line) and annular ducts (symbols: $n = 1$ and $0.1 \leq R \leq 0.99$) (a): $\hat{\tau}_{\rm y} = 1/R$; (b): $\hat{\tau}_{\rm y} = 2/(R+1)$; (c): $\hat{\tau}_{\rm y} = 1$

.

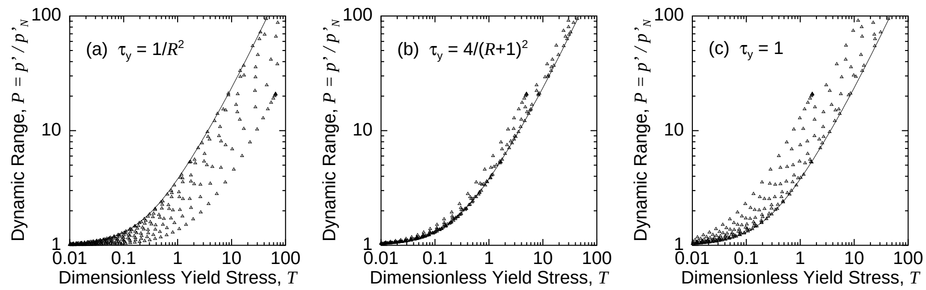

FIG. 5. Poiseuille flow of ER and MR materials through rectangular ducts (solid line) and annular ducts (symbols: $n = 2$ and $0.1 \leq R \leq 0.99$). (a): $\hat{\tau}_{\rm y} = 1/R$; (b): $\hat{\tau}_{\rm y} = (2/(R+1))$; (c): $\hat{\tau}_{\rm y} = 1$

.

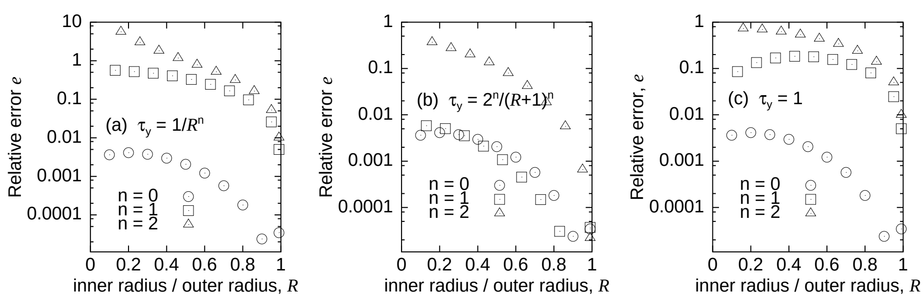

FIG. 6. Relative error of the rectangular duct approximation to the annular duct Poiseuille flow problem. (a): $\hat{\tau}_{\rm y} = 1/R$; (b): $\hat{\tau}_{\rm y} = (2/(R+1))$; (c): $\hat{\tau}_{\rm y} = 1$

.

V. SUMMARY

The yield stresses in ER and MR materials increases monotonically with the applied electric or magnetic field. This yield stress is typically inhomogeneous, due to the migration of particulates away from the walls of the duct and due to the concentration of the field intensity near the inner radius of ducts with annular cross sections. For some /ermr/ materials and devices, the inhomogeneities arising from particle migration due to electrophoresis and inertial lift forces may dominate the inhomogeneities due to nonuniform electric/magnetic fields. Relations incorporating the inhomogeneity due to radial effects and describing the stresses and velocities in annular Poiseuille flows of ER and MR materials are obtained. Given the yield stress, ${\tau_{\mathrm{y}}}^*$, and the plastic viscosity, η^*, the duct radii, R_1^* and R_2^*, the flow rate Q, and the exponent n in the power law relating the yield stress to the electric/magnetic field, the responding pressure gradient may be numerically calculated using the method outlined in section 3. Alternatively, closed form expressions for the Poiseuille flow of Bingham materials flowing through rectangular ducts can accurately describe the annular Poiseuille flow of ER/MR materials, even for non-slender ducts, provided that the homogeneous yield stress is evaluated at the average radius point, $(R_1^* + R_2^*)/2$. The yield stress for the field at mid-gap, balances the high yield stresses at the inner duct wall with the lower yield stresses at the outer duct wall.

VI. ACKNOWLEDGMENTS

This material is based on work supported by the National Science Foundation, Earthquake Hazard Mitigation Program, under Award No. CMS-9624949 and by the Ford Motor Corporation. Any opinions, findings, and conclusions or recommendations expressed in this publication are those of the author and do not necessarily reflect the views of the National Science Foundation or the Ford Motor Corporation.

References

Atkin, R.J., X. Shi, and W.A. Bullough, "Solution of the constitutive equations for the flow of an electrorheological fluid in a radial configuration," J. Rheol. **35**, 1441–1461 (1991).

Bird, R.B., W.E. Stewart, and E.N. Lightfoot, Transport Phenomena Wiley, (1960).

Bird, R.B., G.C. Dai, and B.J. Yaruso, "The Rheology and Flow of Viscoplastic Materials," Reviews in Chemical Engineering **1**, 1–70 (1983).

Burton, S.A., N. Makris, I. Konstantopoulos, and P.J. Antsaklis, "Modeling the Response of ER Damper: Phenomenology and Emulation," J. Eng. Mech. **112**, 886–906 (1996).

Choi, S.B. and W.K. Kim, "Vibration control of a semi-active suspension featuring electrorheological fluid dampers," J. Sound Vib. **234**, 537–546 (2000).

Choi U.S. and B.G. Ahn, "Electrorheology of cellulose phosphate ester suspension as a new anhydrous ER fluid," Colloid Surface A **168**, 71–76 (2000).

Dyke, S.J., B.F. Spencer, and M.K. Sain, "An experimental study of MR dampers for seismic protection," Smart Mat'ls and Structures **7**, 693–703 (1998).

Gamota, D.R. and F.E. Filisko, "Dynamic mechanical studies of electrorheological materials," J. Rheol. **35**, 399–425 (1991).

Gavin, H.P., R.D. Hanson, and F.E. Filisko, "Electrorheological dampers ,Part I:Analysis and Design," J. Appl. Mech. **63**, 669–675 (1996a).

Gavin, H.P., R.D. Hanson, and N.H. McClamroch, "Electrorheological dampers, Part II: Testing and Modeling," J. Appl. Mech. **63**, 676–682 (1996b).

Gavin, Henri P. "The Effect of Particle Concentration Inhomogeneities on the Steady Flow of Electro- and Magneto-Rheological Materials," J. Non-Newtonian Fluid Mech. **71**, 165–182 (1997).

Gavin, H.P. “Design method for high-force electrorheological dampers,” Smart Mat’ls and Structures. **7**, 664–673 (1998).

Gavin, H.P. “Control of Seismically-Excited Vibration using Electrorheological Materials and Lyapunov Methods,” IEEE Trans. Automatic Control. **9**, 27–36 (2001).

Ginder, J.M., L.C. Davis, and L.D. Elie “Rheology of Magnetorheological Fluids: Models and Measurements,” Int’l J. Mod. Phys. B **10**, 3293–3303 (1996).

Huang J., J.G. Guan, and W.Y. Chen “Preparation and magnetorheological properties of aqueous suspension based on emulsion droplets containing Fe3O4 nanoparticles,” J. Wuhan University of Technology, **13**, 1–6 (1998).

Jolly M.R., J.W. Bender and J.D. Carlson, “Properties and applications of commercial magnetorheological fluids,” J. Intelligent Mat’ls Systems and Structures **10**, 5–13 (1999).

Kamath, G.M., M.K. Hurt, and N. Wereley, “Analysis and testing of Bingham plastic behavior in semi-active electrorheological fluid dampers,” Smart Structures and Mat’ls **5**, 576–590 (1996).

Kamath, G.M., N.M. Wereley, and M.R. Jolly, (1999) “Characterization of magnetorheological helicopter lag dampers,” J. Amer. Helicopter Society **44**, 234–248 (1999).

Lindler J. and N.M. Wereley (1999) “Analysis and testing of electrorheological bypass dampers,” J. Intelligent Mat’l Systems and Structures **10**, 363–376 (1999).

Makris, N., S.A. Burton, D. Hill, and M. Jordan, “Analysis and Design of ER Damper for Seismic Protection of Structures,” J. Eng. Mech. **122**, 1003–1011 (1996).

Marksmeier, T.M., F. Gordaninejad and E.L. Wang, “Design and performance of an electrorheological grease ERG shock absorber,” International J. Modern Physics B **13**, 2135–2142 (1999).

Murata, Y. and K. Maemori, “Optimum design of ER dampers for ambulances,” JSME International J. C - Mechanical Systems **42**, 838–846 (1999).

Nguyen, Q.D. and D.V. Boger, “Measuring the Flow Properties of Yield Stress Fluids,” Annual Review of Fluid Mechanics **24**, 47–88 (1992).

Parthasarathy, M. and D. Kingenberg, “Electrorheology: mechanisms and models,” Mat’ls Science and Engineering, R17 57–103 (1996).

Peel, D.J., R. Stanway, and W.A. Bullough, “Dynamic modelling of an ER vibration damper for vehicle suspension applications,” Smart Mat’ls and Structures **5**, 591–606 (1996).

Phillips, R.W. Engineering application of fluids with a variable yield stress. Ph.D. dissertation, Department of Mechanical Engineering, University of California, Berkeley (1969).

Phule, P.P. and J.M. Ginder, “Synthesis and properties of novel magnetorheological fluids having improved stability and redispersibility,” Int’l J. Mod. Phys. B **13**, 2019–2027 (1999).

Quist, G.P. and F.E. Filisko, “ER suspensions with ER active matrix liquids,” Int’l J. Mod. Phys., B **13**, 1675–1681 (1999).

Rajagopal, K.R. and A.S. Wineman, “Flow of electro-rheological materials,” Acta Mechanica **91**, 57–75 (1992).

Rajagopal, K.R., and M. Růžička, “On the Modeling of Electrorheological Materials,” *Mechanics Research Comunications,* **23**, 401–407 (1996).

Rankin, P.J., J.M. Ginder and D.J. Klingenberg, “Electro- and magneto-rheology,” Current Opinion in Colloid and Interface Science **3**, 373–381 (1998).

Shimada, K. and T. Fujita, “A device to regulate rotational speed using a rotating regulator with electrorheological fluid,” Experimental Mechanics **40**, 231–240 (2000).

Sims N.D., D.J. Peel and R. Stanway “The electrorheological long-stroke damper: A new modelling technique with experimental validation,” J. Sound and Vib. **229**, 207–227 (2000).

Trlica J., P. Saha and O. Quadrat, “Electrorheological activity of polyphenylenediamine suspensions in silicone oil,” Physica A **283**, 337–348 (2000).

Wilkinson, W.L. Non-Newtonian Fluids: Fluid Mechanics, Mixing, and Heat Transfer, Pergamon, New York (1960).

Wineman, A.S. and Rajagopal, K.R., “On constitutive equations for electrorheological materials,” Continuum Mechanics and Thermodynamics, **7** 1–22, (1995).

Wu C.W. and H. Conrad, “Electrorheology of suspensions of Si particles with an oxide film in silicone oil,” Int’l J. Mod. Phys. B **13**, 1713–1720 (1999).

Yao, G.Z., F.F. Yap, and G. Chen, “Electro-rheological multi-layer squeeze film damper and its application to vibration control of rotor system,” J. Vib. and Acoustics **122**, 7–11 (2000).